Supporting Information

Self-Sacrificed Synthesis of Carbon-Coated SiO$_x$ Nanowires for High Capacity Lithium Ion Battery Anode

Zhaohuai Li[a], Qiu He[a], Liang He[a*], Ping Hu[a], Wei Li[b], Haowu Yan[a], Xianzhou Peng[a], Congyun Huang[b], and Liqiang Mai[a*]

[a] State Key Laboratory of Advanced Technology for Materials Synthesis and Processing,

Wuhan University of Technology, Wuhan 430070, P. R. China

[b] School of Materials Science and Engineering, Wuhan University of Technology, Wuhan
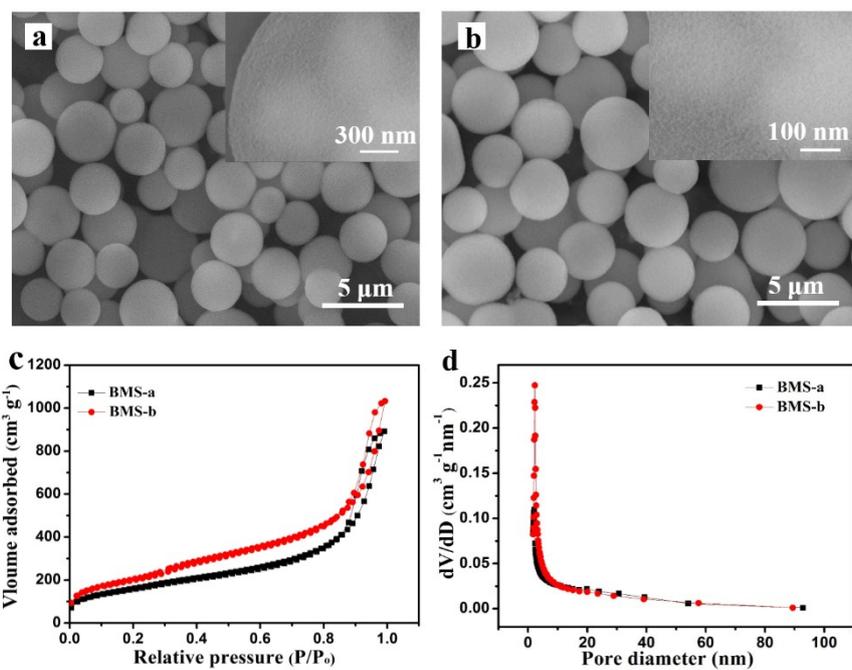
430070, P. R. China

Fig. S1 Typical SEM images of BMS-a (a) and BMS-b (b) (inset is the SEM image with higher magnification), and BJH (c) and pore size distribution curves (d) of BMS-a and BMS-b.
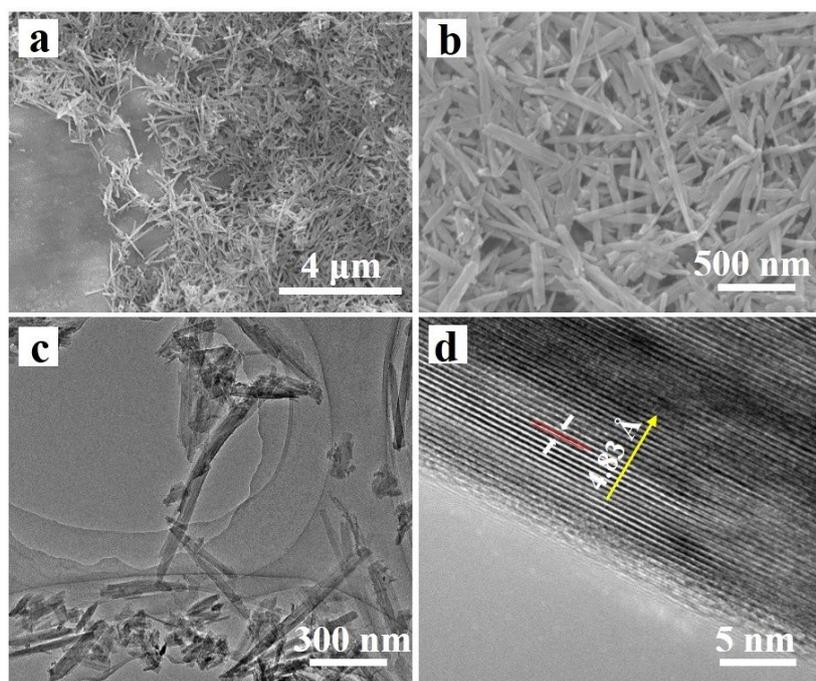

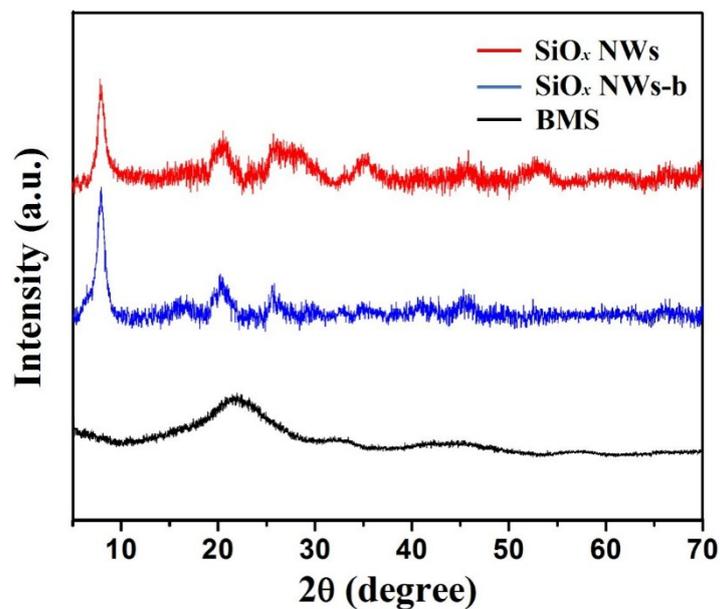**Fig. S2** SEM (a, b), TEM (c) and HRTEM (d) images of SiO$_x$ NWs-b.

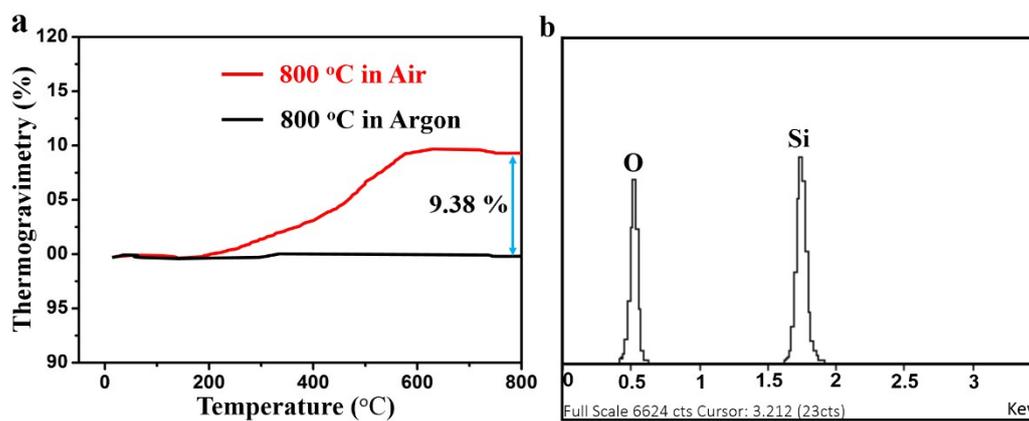**Fig. S3** XRD patterns of BMS precursor and as-synthesized SiO$_x$ NWs.

Fig. S4 (a) TGA curves of SiO$_x$ NWs in air and argon atmosphere (flow of 100 ml/min and a heating rate of 10 °C/min). (b) The EDS of SiO$_x$ NWs after annealing in air at 800 °C. The concentration of oxygen vacancies is calculated from the difference in weight increase between the two TGA curves.
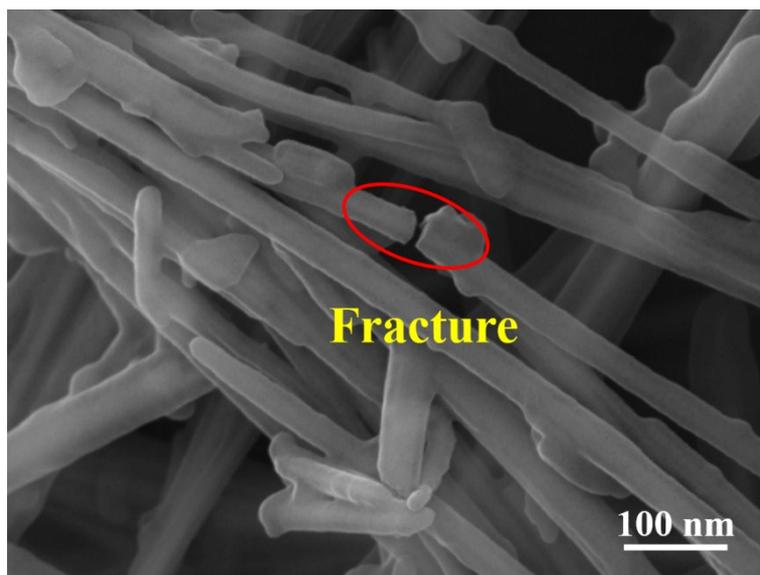
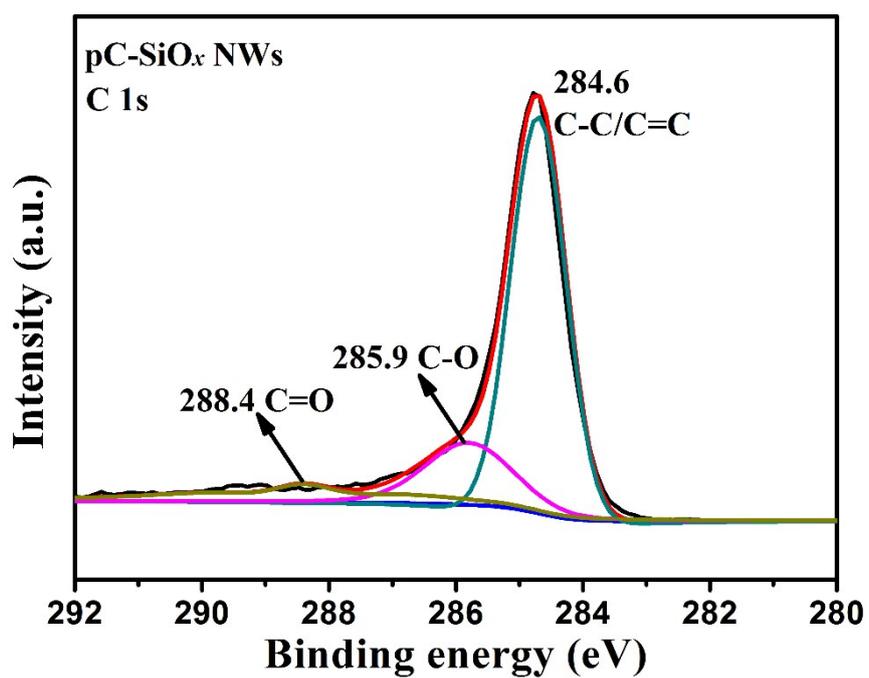**Fig. S5** Typical SEM image of RF-SiO$_x$ NWs. The area marked by red circle shows the existance of fracture in RF-SiO$_x$ NWs.

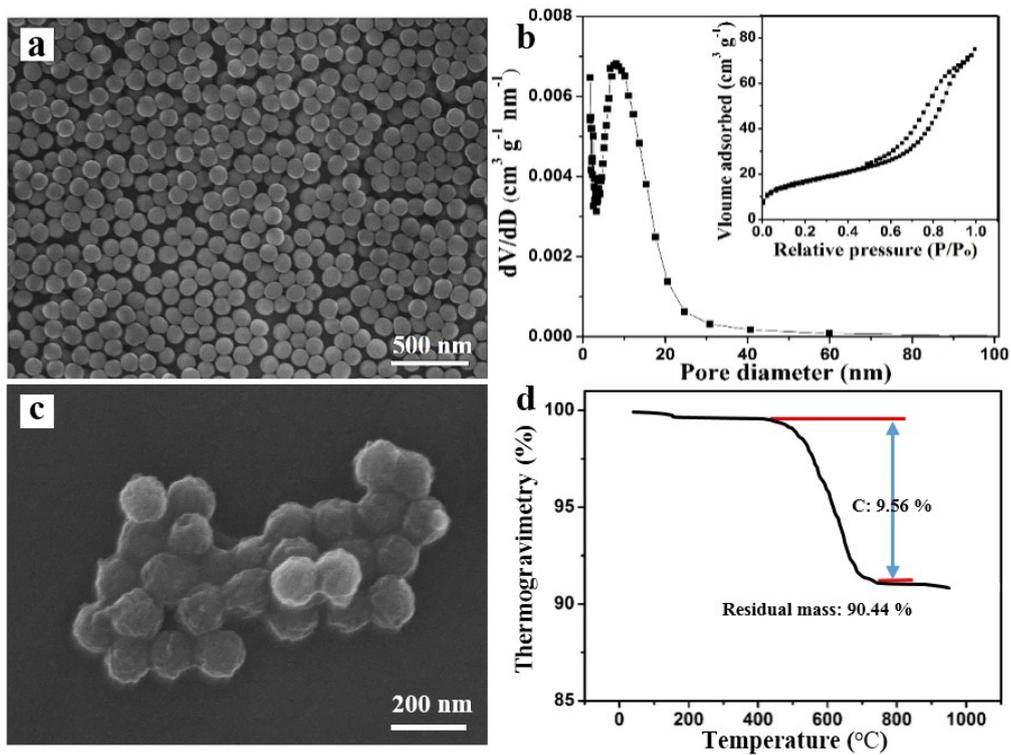**Fig. S6** High-resolution C 1s XPS spectrum of pC-SiO$_x$ NWs.

Fig. S7 (a) SEM image of p-SiO$_2$ NPs and (b) corresponding BET curves. (c) SEM image of pC-p-SiO$_2$ NPs and (d) corresponding TGA profile.
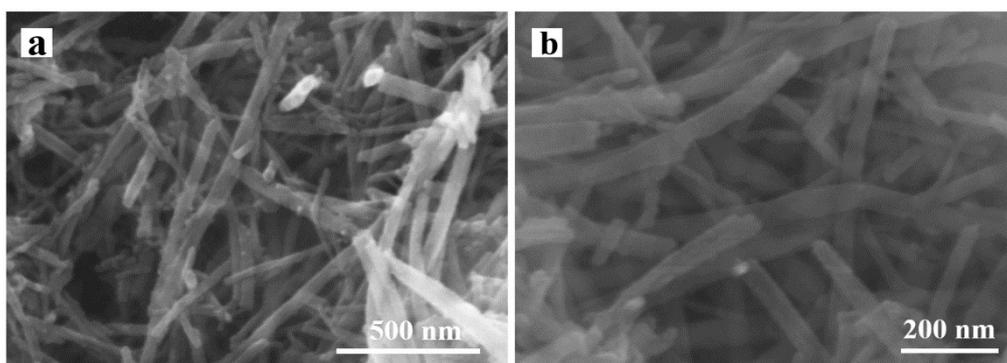

Fig. S8 SEM images of pC-SiO$_x$ NWs after 150 electrochemical cycles at a current density of 500 mA g^{-1}.